

Quantized Control for Input-to-State Stabilization of Discrete-Time Markov Jump Systems with Coding and Decoding Procedures

Xiaohui Gao, Yue Su, Chengyi Han, Jing Han, and Yebin Chen

Abstract—This paper investigates the input-to-state stabilization of discrete-time Markov jump systems. A quantized control scheme that includes coding and decoding procedures is proposed. The relationship between the error in the system state before and after encoding and decoding, the quantization range, and the packet length is established. A criterion for input-to-state stability of the quantized closed-loop Markov jump system is obtained using a Lyapunov function and the Schur complement. The gains of the required quantized controller can be derived from a feasible solution to linear matrix inequalities. Finally, the proposed control scheme is validated using an operational amplifier circuit system.

Index Terms—Markov jump system, Input-to-state stability, Quantized control, Coding-decoding procedure.

I. INTRODUCTION

MARKOV jump systems (MJSs) consist of multiple subsystems and a Markov chain that governs the transitions of the system. Such systems are particularly effective for characterizing the dynamics of systems that exhibit sudden and unpredictable alterations in their parameters or underlying structure [1–3]. Applications of MJSs span various fields, including power system security [4], secure chaotic communication [5], oil price analysis [6], the spread of infectious diseases [7], and automotive power-train control [8]. MJSs can be categorized into continuous-time models and discrete-time models, with the latter comprising discrete-time subsystems. Discrete-time MJSs may be preferred over continuous-time ones because they can be implemented more straightforwardly using digital hardware [9].

As network technology advances, networked control systems enable remote control for distributed devices. Within these systems, each device is connected through networks and passes data transmission and control commands to the target device [10, 11]. Typically, analog signals must undergo sampling, quantization, and encoding before they can be

converted into digital signals for digital communication. Sampling and quantization processes capture the time and amplitude of a discrete signal from its analog counterpart, whereas encoding converts the results of quantization into corresponding binary codes [12]. As network resources are restricted, signal transmission is affected by channel throughput. Quantizing the signal to be transmitted can effectively deal with this problem [13]. Quantizers that produce quantized signals include static and dynamic quantizers. Unlike static quantizers, dynamic ones can adjust quantization parameters dynamically to prevent saturation [14, 15]. Using quantization measurements and input mode correlation interval time delay, Liu et al. [16] considered the dynamic output-feedback control for MJSs. In [17], Yang et al. studied the problem of quantized control for MJSs with time delays and partially known transfer probabilities. Zong et al. [18] explored finite-time control strategies for MJSs with dynamic quantization driven by an event-triggered approach. Recently, Zhou et al. [19] introduced quantized control schemes aimed at achieving input-to-state stabilization of MJSs under multi-mode injection attacks.

It is worthwhile to note that the controlled plants in [16–19] are continuous-time MJSs. Furthermore, most existing studies on MJSs under quantized control do not include considerations of coding and decoding procedures. In the process of data transmission through networks, coding and decoding procedures can compress and encrypt data to reduce transmission bandwidth and storage space requirements [20]. In [21], Dey et al. explored how to develop encoding and decoding strategies for the linear control of linear systems with a wireless communication link between the estimator and the sensor. Yan et al. [22] proposed an observer-based endec decoder using dynamic uniform quantization to tackle the N-step model predictive control problem in networked control systems with constrained communication capabilities. In [23], Wakaiki proposed a joint design approach utilizing a coding scheme while was proposed to examine the self-triggered stability of discrete-time linear systems that depend on quantized state measurements. Tao et al. [24] explored the problem associated with quantized iterative learning control by implementing encoding and decoding techniques in networked control systems facing communication limitations. In [25], Li et al. introduced a coding and decoding scheme that utilizes dynamic quantization for discrete-time systems subject to norm-bounded uncertainties, examining how coding length affects system performance. To our knowledge, nevertheless, very little research has been done on quantized control for MJSs with coding and decoding procedures, especially in the discrete-time scenario.

Manuscript received May 15, 2024; revised November 6, 2024. This work was supported by the Natural Science Foundation of the Anhui Higher Education Institutions (Grant No. 2022AH050310).

Xiaohui Gao is a postgraduate student at the School of Computer Science and Technology, Anhui University of Technology, Ma'anshan 243032, China (e-mail: gaohx@ahut.edu.cn).

Yue Su is a postgraduate student at the School of Computer Science and Technology, Anhui University of Technology, Ma'anshan 243032, China (e-mail: ysu@ahut.edu.cn).

Chengyi Han is a postgraduate student at the School of Computer Science and Technology, Anhui University of Technology, Ma'anshan 243032, China (e-mail: hanchengyi@ahut.edu.cn).

Jing Han is a teaching assistant of the School of Electrical and Information Engineering, Wanjiang University of Technology, Ma'anshan 243032, China (e-mail: jing130_han@163.com).

Yebin Chen is a full professor at the School of Computer Science and Technology, Anhui University of Technology, Ma'anshan 243032, China (e-mail: cyb7102@163.com).

Motivated by the above discussion, this work investigates the problem of input-to-state stabilization of discrete-time MJSs. A quantized control scheme with coding and decoding procedures is proposed. The relationships between the error in the system state before and after encoding and decoding, the quantization range, and the packet length are established. A criterion for input-to-state stability (ISS) of the quantized closed-loop system is obtained using a Lyapunov function and the Schur complement. The gains of the required quantized controller can be obtained from a feasible solution of linear matrix inequalities (LMIs). Finally, the proposed method is validated using an operational amplifier circuit system.

Notation. In this paper, the notation \mathbb{R}^a refers to an a -dimensional real vector space. The Euclidean vector norm is represented by $\|\cdot\|$, while $\sup\{\cdot\}$ denotes the supremum, and $\lambda_{\min}(\cdot)$ and $\lambda_{\max}(\cdot)$ are used to represent the minimum and maximum eigenvalues. The term $He\{Q\}$ refers to the sum of the matrix Q and its transpose. The notation $diag\{\cdot\}$ indicates a block-diagonal matrix, and $\mathbb{E}\{\cdot\}$ denotes the expected value operator. For any matrix $Q > 0$, this means that Q is symmetric positive-definite. The symbol “*” represents a symmetry block in a square matrix.

II. PRELIMINARIES

A. System model

Consider the following discrete-time MJS:

$$x(k+1) = A_{\delta(k)}x(k) + B_{\delta(k)}u(k) + D_{\delta(k)}w(k), \quad (1)$$

where $x(k) \in \mathbb{R}^{n_x}$, $u(k) \in \mathbb{R}^{n_u}$, and $w(k) \in \mathbb{R}^{n_w}$ mean the state, control input, and external disturbance, respectively. Matrices $A_{\delta(k)}$, $B_{\delta(k)}$, and $D_{\delta(k)}$ denote the given system parameters, where $\delta(k)$ is determined by a Markov jump process that utilizes a transition probability matrix denoted as $\Psi = (\varphi_{ij})_{n \times n}$,

$$\varphi_{ij} = \Pr\{\delta(k+1) = j \mid \delta(k) = i\}, \quad i, j \in \mathcal{N} \quad (2)$$

for $\varphi_{ij} \in [0, 1]$ [26–28], which satisfies

$$\sum_{j=1}^n \varphi_{ij} = 1, \quad \forall i, j \in \mathcal{N} = \{1, 2, \dots, n\}.$$

B. Dynamic quantizer

Now, assume that the system state $x(k)$ undergoes uniform quantization before passing through the communication network. We recall the uniform quantization process and then apply it to the coding and decoding procedures. For the system state $x(k)$ to be quantized, there exists the quantization error bound $\Theta > 0$ and quantization range $\Lambda > 0$ to satisfy the following conditions:

$$\|q(x(k)) - x(k)\| \leq \Theta, \quad \|x(k)\| \leq \Lambda, \quad (3)$$

$$\|q(x(k)) - x(k)\| > \Theta, \quad \|x(k)\| > \Lambda. \quad (4)$$

The range of quantization error described in (3) applies when the quantizer is not in a state of saturation, while the condition in (4) suggests a feasible way to detect whether saturation is occurring.

Unlike the static quantizers with a fixed saturation threshold [29–31], we propose the use of a dynamic parameter

$\mu(k) > 0$ within the uniform quantizer $q_{\mu(k)}(x(k))$. This adaptation allows for an expanded quantization range and a reduced bound on quantization error as described in (18) and (23):

$$q_{\mu(k)}(x(k)) = q(v(k))\mu(k), \quad v(k) = \frac{x(k)}{\mu(k)}. \quad (5)$$

Based on the above two conditions, the following modifications are made:

$$\begin{aligned} \|q_{\mu(k)}(x(k)) - x(k)\| &\leq \Theta\mu(k), & \|x(k)\| &\leq \Lambda\mu(k), \\ \|q_{\mu(k)}(x(k)) - x(k)\| &> \Theta\mu(k), & \|x(k)\| &> \Lambda\mu(k). \end{aligned}$$

With no saturation, the quantization error $e(k)$ of the dynamic quantizer is in the range of $[-\Theta\mu(k), \Theta\mu(k)]$ [32–34]. In cases of positive or negative saturation, we set the quantization state to be fixed to the maximum or minimum value that the quantizer can represent.

In dynamic quantizer (5), the interval $[-\Lambda, \Lambda]$ is partitioned into β regions subject to

$$v(k) \in \mathcal{R}_\tau = \left[-\Lambda + \frac{2(\tau-1)\Lambda}{\beta}, -\Lambda + \frac{2\tau\Lambda}{\beta}\right),$$

with $\tau \in \{1, 2, \dots, \beta\}$, and the quantized state $q(v(k))$ is denoted by:

$$q(v(k)) = -\Lambda + \frac{(2\tau-1)\Lambda}{\beta}. \quad (6)$$

Taken together, when the quantized state $v(k)$ lies in the region $[-\Lambda, \Lambda]$, the quantization error satisfies the following condition:

$$\|q(v(k)) - v(k)\| \leq \Theta = \frac{\Lambda}{\beta}. \quad (7)$$

In the case where the quantizer (5) is not saturated, a state-dependent adjustment strategy for the quantization parameters is introduced due to the limited network resources. In the case the quantizer (5) is saturated, the quantization parameter cannot be infinitely small due to the limitation of the network resources, and the minimum quantization parameter is:

$$\theta_1 \|x(k)\| \leq \mu(k) \leq \theta_2 \|x(k)\|, \quad \text{if } \|x(k)\| \geq \Lambda\phi_{\min}, \quad (8)$$

$$\mu(k) = \phi_{\min}, \quad \text{if } \|x(k)\| < \Lambda\phi_{\min}, \quad (9)$$

where $\Lambda\phi_{\min}$ is the minimum quantization region, and the parameters θ_1 and θ_2 satisfy the condition $\theta_1 = \frac{1}{2}\theta_2$. Specific adjustment strategies for the quantizer parameters to ensure that $\mu(k)$ satisfies conditions (8) and (9) are given below:

$$\mu(k) = \begin{cases} 2^h, & \text{if } \|x(k)\| \geq \Lambda\phi_{\min} \\ 2^{-l}, & \text{if } \|x(k)\| < \Lambda\phi_{\min} \end{cases} \quad (10)$$

where

$$h = \begin{cases} j_l, & \text{if } \theta_1 \|x(k)\| > 1 \\ 0, & \text{if } \theta_1 \|x(k)\| \leq 1 \leq \theta_2 \|x(k)\| \\ -l, & \text{if } \theta_2 \|x(k)\| < 1 \end{cases} \quad (11)$$

with

$$j_l = \max \{j_l \in J \mid \theta_2 \|x(k)\| \times 2^{-j_l} \geq 1\} \quad (12)$$

$$l_l = \min \{l_l \in L \mid \theta_2 \|x(k)\| \times 2^{l_l} \geq 1\} \quad (13)$$

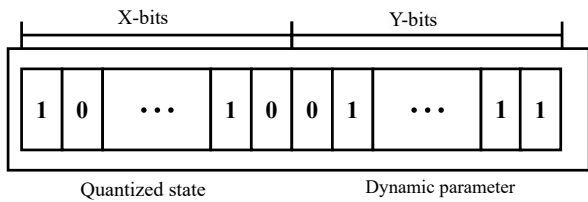


Fig. 1. The bits allocation.

and $J = \{1, 2, \dots, \bar{j}_i\}$, $L = \{1, 2, \dots, \bar{l}_i\}$. The parameters \bar{j}_i and \bar{l}_i are the maximum and minimum values for the integer h , respectively. The minimum quantizer's parameter is

$$\phi_{min} = \min\{\mu(k)\} = 2^{-\bar{l}_i}.$$

When

$$\|x(k)\| \geq \Lambda\phi_{min},$$

the dynamic quantizer's parameter $\mu(k)$ satisfies (11). By similar lines to [25], (11) can be ensured.

C. Coding procedure

The signal to be encoded has the following two components, including the quantization state $q(v(k))$ and the dynamic quantizer parameter $\mu(k)$. The quantization process maps the signal to a discrete set of ranges of values, which are subsequently encoded into a binary string by the encoder:

$$\begin{aligned} \check{x}(k) &= f(q_{\mu(k)}(x(k))) = \tilde{x}(k)\tilde{\mu}(k) \\ &= m(q(v(k)))g(\mu(k)). \end{aligned} \quad (14)$$

The quantizer (5) maps the quantized state signals $\tilde{x}(k)$ by the corresponding encoder function to a finite number of discrete values $\tau \in \{1, 2, \dots, \beta\}$

$$\tilde{x}(k) = m(q(v(k))) = \tau, \quad \text{if } v(k) \in \mathcal{R}_\tau,$$

Then, according to the adjusting rules (10)-(13), the quantizer maps the adaptive quantization parameter $\mu(k)$ via the encoder function $g(\mu(k))$ as:

$$\tilde{\mu}(k) = g(\mu(k)) = \begin{cases} h, & \text{if } \|x(k)\| \geq \Lambda\phi_{min} \\ -\bar{l}_i, & \text{if } \|x(k)\| < \Lambda\phi_{min} \end{cases} \quad (15)$$

It is assumed that the encoded quantization state $\tilde{x}(k)$ and the encoded dynamic parameters $\tilde{\mu}(k)$ are represented using X -bits and Y -bits, respectively. Thus, the length of the whole packet is $(X + Y)$ -bits. The packet lengths for the quantized state and dynamic parameters by binary coding are shown in Fig. 1.

In this paper, X is viewed as the minimum number of bits required to encode the integer β and the number β of quantization level determined by:

$$\beta = 2^X. \quad (16)$$

Based on (10), (11), and (15), we can conclude that $\tilde{\mu}(k) \in \{-\bar{l}_i, \dots, 0, \dots, \bar{j}_i\}$. Because the coding length of $\tilde{\mu}(k)$ is Y -bits, the selection of parameters \bar{l}_i and \bar{j}_i meets the requirements:

$$\bar{l}_i + \bar{j}_i + 1 = 2^Y. \quad (17)$$

Ensure that the quantizer does not saturate by setting

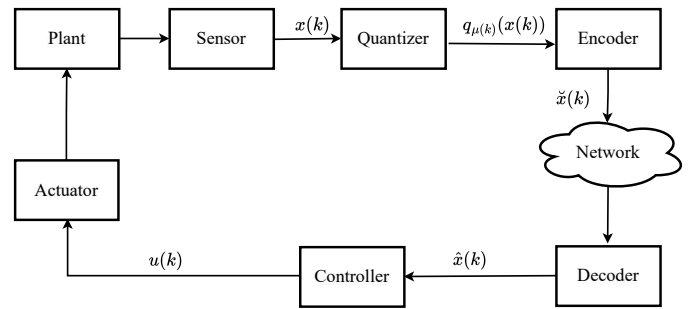


Fig. 2. The framework of the system model under the controller.

the parameter of the quantizer $\phi_{max} = \max\{\mu(k)\}$ large enough, i.e., $\|x(k)\| < \Lambda\phi_{max}$. The maximum coding range is denoted as:

$$\Lambda_{max} = \Lambda\phi_{max} = 2^{\bar{j}_i} \Lambda. \quad (18)$$

D. Decoding procedure

The decoder converts the received digital signal into an analog signal, and the decoding function at the controller side is constructed as follows:

$$\begin{aligned} \hat{x}(k) &= f^{-1}(\check{x}(k)) = m^{-1}(\check{x}(k))g^{-1}(\tilde{\mu}(k)) \\ &= q(v(k))\mu(k). \end{aligned} \quad (19)$$

Remark 1. It can be seen from (14) and (19) that the encoding and decoding processes are reciprocal, i.e., $\check{x}(k) = \hat{x}(k)^{-1}$. The encoding process converts the original information into a digital form suitable for storage, transmission, and processing. The decoding process converts the received digital signal back to the original data to maintain the integrity and consistency of the overall information.

E. Problem statement

The controller $u(k)$ is given by

$$u(k) = K_{\delta(k)}\hat{x}(k), \quad (20)$$

where $K_{\delta(k)} \in \mathbb{R}^{n_u \times n_x}$ is the control gain to be designed later.

Combining system (1) with controller (20), the quantized closed-loop system can be obtained as:

$$\begin{aligned} x(k+1) &= A_{\delta(k)}x(k) + B_{\delta(k)}u(k) + D_{\delta(k)}w(k) \\ &= A_{\delta(k)}x(k) + B_{\delta(k)}K_{\delta(k)}\hat{x}(k) + D_{\delta(k)}w(k) \\ &= (A_{\delta(k)} + B_{\delta(k)}K_{\delta(k)})x(k) \\ &\quad + B_{\delta(k)}K_{\delta(k)}e(k) + D_{\delta(k)}w(k), \end{aligned} \quad (21)$$

where

$$e(k) = \hat{x}(k) - x(k) = q(v(k))\mu(k) - x(k). \quad (22)$$

The framework of the quantized closed-loop system is shown in Fig. 2.

For the error $e(k)$ in the system state before and after encoding and decoding, as derived from formulas (16), (17), and (22), we can obtain

$$e(k) \leq \Lambda\phi_{min} = 2^{-X-2^{-\bar{l}_i}} \Lambda. \quad (23)$$

Remark 2. Through (23), the relationship between the error in the system state before and after encoding and decoding,

the quantization range, and the packet length can be established by following a given minimum error bound. When the coding length X increases, the error $e(k)$ in the system state before and after encoding and decoding decreases. To investigate the effect of length of the whole packet on the error $e(k)$ in the system state before and after encoding and decoding, we keep the minimum value of the dynamic quantizer parameter $\min\{\mu(k)\} = 2^{-\bar{l}_i}$, and the quantization range Λ fixed, and observe its effect on the error while varying the length X .

Definition 1. [19] If there are functions $\theta_1(s) \in \mathcal{K}$ and $\theta_2(s, k) \in \mathcal{KL}$ such that for any initial state $x(0)$ and external disturbance $w(k) \in \mathbb{R}^{n_w}$, the state $x(k)$ exists for all $k \geq 0$ and fulfills the following inequality:

$$\mathbb{E}\{\|x(k)\|\} \leq \theta_1\left(\sup_{0 < s < k}\{\|w(s)\|\}\right) + \mathbb{E}\{\theta_2(\|x(0), k\|\}\},$$

then the closed-loop system is deemed to exhibit ISS.

Now, the objective of this work can be accurately stated as follows: For the discrete-time MJS, design a quantized controller (20) with coding and decoding procedures to ensure that the closed-loop system (21) has ISS.

III. MAIN RESULTS

To propose our main results, which rely on the following lemmas:

Lemma 1. [35] For a real scalar $\zeta > 0$ and matrices W_1 and W_2 with appropriate dimensions

$$W_1^T W_2 + W_2^T W_1 \leq \zeta W_1^T W_1 + \zeta^{-1} W_2^T W_2,$$

hold.

Lemma 2. [36] Given symmetric matrices

$$H = \begin{bmatrix} H_{11} & H_{12} \\ * & H_{22} \end{bmatrix},$$

which H_{11} is $n \times n$ dimensional, the following three conditions are equivalent:

- (i) $H < 0$;
- (ii) $H_{11} < 0, H_{22} - H_{12}^T H_{11}^{-1} H_{12} < 0$;
- (iii) $H_{22} < 0, H_{11} - H_{12}^T H_{22}^{-1} H_{12} < 0$.

Lemma 3. [37] For any two matrices Z_1 and Z_2 with appropriate dimensions

$$-Z_1^T Z_2^{-1} Z_1 \leq Z_2 - Z_1^T - Z_1,$$

hold true.

Lemma 4. [38] For two random variables X and Y , the law of total expectation can be expressed as:

$$\mathbb{E}\{\mathbb{E}\{Y|X\}\} = E\{Y\}.$$

We study the analysis of the ISS of closed-loop system (21) with coding and decoding procedures and present the following sufficient condition:

Lemma 5. Given constants $\zeta > 0, \Theta > 0$, if there exist scalars $\theta_2 > 0, \rho > 0, \lambda_{min}(P) > 0$, and $\lambda_{max}(P) > 0$, and matrices $P_i > 0$ and $K_i, i \in \mathcal{N}$ such that

$$\Lambda\theta_2 \geq 2, \tag{24}$$

$$\lambda_{min}(P)I_{2n_x} < P_i < \lambda_{max}(P)I_{2n_x}, \tag{25}$$

$$\Upsilon = \tilde{P} + (1 + \zeta)\hat{A}_i^T \bar{P}_i \hat{A}_i < 0, \tag{26}$$

hold, where

$$\tilde{P} = \text{diag}\{-P_i + 2\rho\Theta^2\theta_2^2, -\rho I\},$$

$$\hat{A}_i = [A_i + B_i K_i \quad B_i K_i], \bar{P}_i = \sum_{j=1}^n \pi_{ij} P_j.$$

Then, the quantization controller in (20) can ensure that the closed-loop system (21) has ISS.

Proof: Firstly, it is found from (10)-(13) that

$$\begin{cases} \mu(k) \geq \theta_1 \|x(k)\|, & \|x(k)\| \geq \Lambda\phi_{min} \\ \mu(k) = \phi_{min} > \theta_1 \|x(k)\|, & \|x(k)\| < \Lambda\phi_{min} \end{cases} \tag{27}$$

When $\|x(k)\| < \Lambda\phi_{min}$, according to (10)-(13), we have

$$\theta_1 \|x(k)\| < \phi_{min} < \theta_2 \|x(k)\|.$$

Then, the error $e(k)$ in the system state before and after encoding and decoding is analyzed in two cases:

Case I: $\|x(k)\| \geq \Lambda\phi_{min}$

In this case, due to

$$\mu(k) \leq \theta_2 \|x(k)\|, \|e(k)\| \leq \Theta\mu(k),$$

one has

$$\|e(k)\| \leq \|\Theta\mu(k)\| \leq \|\Theta\theta_2 x(k)\|.$$

Case II: $\|x(k)\| < \Lambda\phi_{min}$

In this case, due to

$$\min\{\mu(k)\} = \phi_{min},$$

one has

$$\|e(k)\| \leq \|\Theta\phi_{min}\| \leq \|\Theta\theta_2 x(k)\|.$$

We derive the following by merging Cases I and II:

$$\begin{aligned} e^T(k)e(k) &\leq x^T(k)\Theta^2\theta_2^2 x(k) + \phi_{min}^T \Theta^2 \phi_{min} \\ &\leq 2x^T(k)\Theta^2\theta_2^2 x(k). \end{aligned} \tag{28}$$

Now, we select the Lyapunov function as:

$$V(k) = x^T(k)P_{\delta(k)}x(k). \tag{29}$$

Utilizing the law of total expectation as demonstrated in Lemma 4, we can drive from equations (2) and (29) that

$$\begin{aligned} &\mathbb{E}\{\Delta V(x(k), \delta(k) = i)\} \\ &= \mathbb{E}\{V(x(k+1), \delta(k+1)) - V(x(k), \delta(k) = i)\} \\ &= \mathbb{E}\left\{\mathbb{E}\{V(x(k+1), \delta(k+1)) | x(k), \delta(k) = i\} \right. \\ &\quad \left. - V(x(k), \delta(k) = i)\right\} \\ &= \mathbb{E}\left\{\sum_{j=1}^n Pr\{\delta(k+1) = j | \delta(k) = i\} x^T(k+1)P_j \right. \\ &\quad \left. x(k+1) - x^T(k)P_i x(k)\right\} \\ &= \mathbb{E}\left\{\sum_{j=1}^n \pi_{ij} x^T(k+1)P_j x(k+1) - x^T(k)P_i x(k)\right\} \\ &= \mathbb{E}\{x^T(k+1)\bar{P}_i x(k+1) - x^T(k)P_i x(k)\} \end{aligned}$$

$$= \eta^T(k) \hat{A}_i^T \bar{P}_i \hat{A}_i \eta(k) + He\{\eta^T(k) \hat{A}_i^T \bar{P}_i D_i w(k)\} + w^T(k) D_i^T \bar{P}_i D_i w(k) - x^T(k) P_i x(k).$$

By utilizing Lemma 1, which can be reformulated as:

$$\eta^T(k) \hat{A}_i^T \bar{P}_i D_i w(k) + w^T(k) D_i^T \bar{P}_i \hat{A}_i \eta(k) \leq \zeta \eta^T(k) \hat{A}_i^T \bar{P}_i \hat{A}_i \eta(k) + \zeta^{-1} w^T(k) D_i^T \bar{P}_i D_i w(k). \quad (30)$$

Then, from (28) and (30) we have

$$\begin{aligned} & \mathbb{E}\{\Delta V(x(k), \delta(k) = i)\} \\ & \leq \eta^T(k) \left(\bar{P} + (1 + \zeta) \hat{A}_i^T \bar{P}_i \hat{A}_i \right) \eta(k) \\ & \quad + (1 + \zeta^{-1}) w^T(k) D_i^T \bar{P}_i D_i w(k) \\ & \quad + 2\rho x^T(k) \Theta^2 \theta_2^2 x(k) - \rho e^T(k) e(k) \\ & \leq \eta^T(k) \Upsilon \eta(k) + (1 + \zeta^{-1}) w^T(k) D_i^T \bar{P}_i D_i w(k) \\ & \leq (1 + \zeta^{-1}) w^T(k) D_i^T \bar{P}_i D_i w(k) \\ & \leq \psi w^T(k) w(k), \end{aligned}$$

where

$$\begin{aligned} \bar{P} &= \text{diag}\{-P_i, 0\}, \quad \eta(k) = [x^T(k) \ e^T(k)]^T, \\ \psi &= \sup_{i \in \mathcal{N}} (\lambda_{\max}((1 + \zeta^{-1}) D_i^T \bar{P}_i D_i)). \end{aligned}$$

We can have

$$\begin{aligned} & \lambda_{\min}(P) \mathbb{E}\{\|x(k)\|^2\} \\ & \leq \mathbb{E}\{V(x(k), \delta(k))\} \\ & \leq \mathbb{E}\{V(x(0), \delta(0))\} + \mathbb{E}\left\{\sum_{s=0}^k \Delta V(x(s), \delta(s))\right\} \\ & \leq \mathbb{E}\left\{x^T(0) P_i x(0) + \sum_{s=0}^k \{\psi w^T(s) w(s)\}\right\} \\ & \leq \lambda_{\max}(P) \mathbb{E}\{\|x(0)\|^2\} + \sup_{0 < s < k} \{\psi w^T(s) w(s)\}, \end{aligned}$$

which means

$$\begin{aligned} & \mathbb{E}\{\|x(k)\|\} \\ & \leq \sqrt{\frac{\lambda_{\max}(P)}{\lambda_{\min}(P)}} \mathbb{E}\{\|x(0)\|\} + \sqrt{\frac{\psi}{\lambda_{\min}(P)}} \sup_{0 < s < k} \{\|w(s)\|\}. \end{aligned}$$

From this and Definition 1, we can determine the ISS. ■

Now, we provide feasible solutions based on certain inequality methods to ensure the stability analysis of Lemma 5 in (24) and (26). Next, we present the following result regarding the ISS synthesis:

Theorem 1. Given constants $\zeta > 0$, $\Theta > 0$, if there exist scalars $\theta_2 > 0$, $\rho > 0$, $\lambda_{\min}(P) > 0$, and $\lambda_{\max}(P) > 0$, and matrices $\hat{P}_i > 0$ and K_i , $i \in \mathcal{N}$ such that (25), and

$$2\rho - \bar{\theta}_2 \Lambda < 0, \quad (31)$$

$$\begin{bmatrix} \hat{P}_i - 2I & 0 & \Upsilon_1 & \sqrt{2}\Theta\bar{\theta}_2 \\ * & -\rho I & \Upsilon_2 & 0 \\ * & * & -(1 + \zeta)^{-1}P & 0 \\ * & * & * & -\rho I \end{bmatrix} < 0, \quad (32)$$

hold, where

$$\begin{aligned} \bar{\theta}_2 &= \rho\theta_2, \\ P &= \text{diag}\{\hat{P}_1, \hat{P}_2, \dots, \hat{P}_n\}, \end{aligned}$$

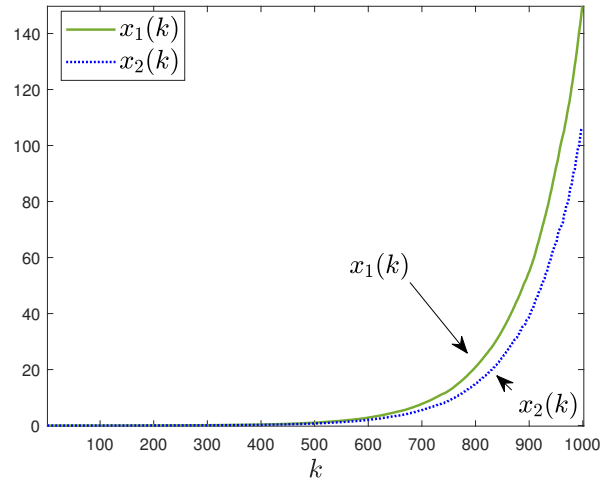


Fig. 3. State trajectories of the open-loop system.

$$\begin{aligned} \Upsilon_1 &= \begin{bmatrix} \sqrt{\pi_{i1}}(A_i + B_i K_i) & \sqrt{\pi_{i2}}(A_i + B_i K_i) \dots \\ \sqrt{\pi_{in}}(A_i + B_i K_i) \end{bmatrix}, \\ \Upsilon_2 &= \begin{bmatrix} \sqrt{\pi_{i1}}(B_i K_i) & \sqrt{\pi_{i2}}(B_i K_i) \dots \\ \sqrt{\pi_{in}}(B_i K_i) \end{bmatrix}. \end{aligned}$$

Then, the quantized closed-loop system (21) has ISS. Furthermore, the gains K_i of the required quantized controller in (20) can be obtained from a feasible solution of LMIs.

Proof: The equivalence between (24) and (31) can be seen by taking $\bar{\theta}_2 = \rho\theta_2$. Next, we show that (26) can be guaranteed by (32). Denote $\hat{P}_i = P_i^{-1}$ by Lemma 3, and notice that the inequality

$$(I - P_i) \hat{P}_i (I - P_i)^T = P_i + \hat{P}_i - 2I \geq 0,$$

holds, which implies

$$-\hat{P}_i \leq P_i - 2I. \quad (33)$$

By (33), the following inequality can be obtained from (32):

$$\begin{bmatrix} -P_i & 0 & \Upsilon_1 & \sqrt{2}\Theta\bar{\theta}_2 \\ * & -\rho I & \Upsilon_2 & 0 \\ * & * & -(1 + \zeta)^{-1}P & 0 \\ * & * & * & -\rho I \end{bmatrix} < 0, \quad (34)$$

where

$$P = \text{diag}\{P_1, P_2, \dots, P_n\}.$$

Then, with (34) and Lemma 2, we can obtain (26). Thus, all the conditions in Lemma 5 hold true, confirming that the quantized closed-loop system (21) has ISS. ■

IV. EXAMPLE

Considering the operational amplifier (OPA) circuit system in [39] and applying Kirchoff's current law to v_1 and v_2 based on the features of their "virtual short" and "virtual off," we obtain the following equation of state:

$$\begin{aligned} \dot{v}_1 &= -\frac{1}{R_1 C_1} v_1 + \frac{1}{R_1 C_1} v_2, \\ \dot{v}_2 &= \frac{1}{R_1 C_2} v_1 + \left(\frac{R_3}{R_2 R_4 C_2} - \frac{1}{R_1 C_2} \right) v_2 - \frac{R_3}{R_2 R_4 C_2} u. \end{aligned}$$

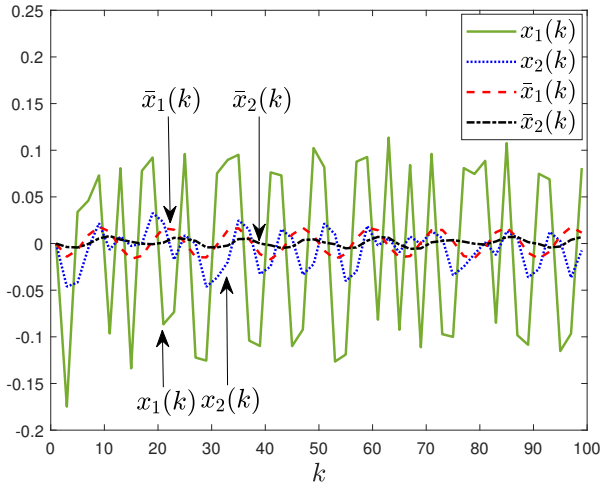


Fig. 4. The system state with quantized under code length $Y = 2$ and $Y = 4$.

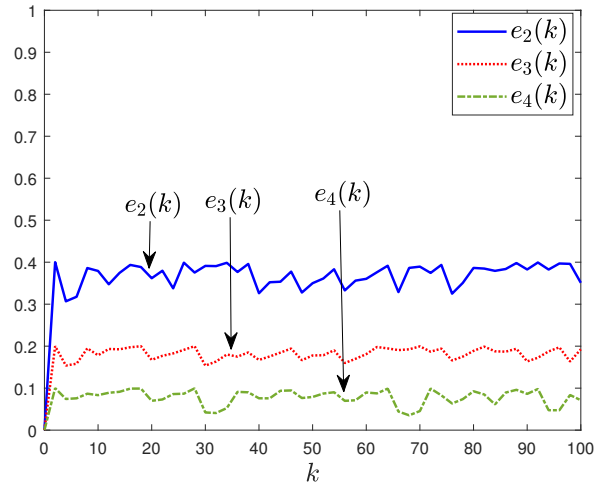


Fig. 6. The error $e_2(k)$, $e_3(k)$, $e_4(k)$ with quantized under the coding length $X = 2, 3, 4$.

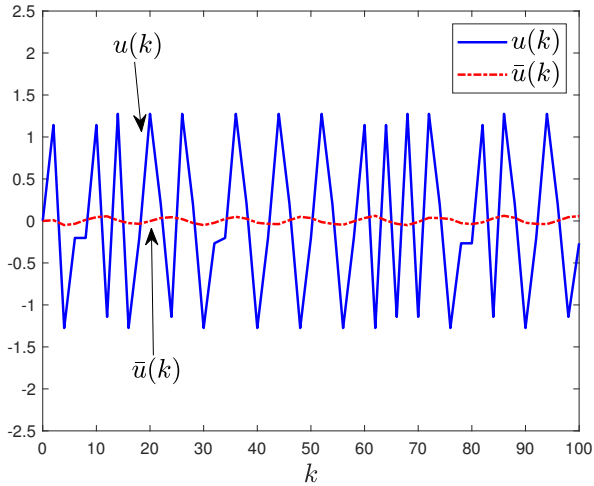


Fig. 5. The control input with quantized under the coding length $Y = 2$ and $Y = 4$.

Define $x_1(k) = v_1$ and $x_2(k) = v_2$. Assuming that C_2 is a small "parasitic" capacitance, it can be considered a perturbation parameter, i.e., $C_2 = \epsilon$, which is taken as $\epsilon_1 = 0.1$ and $\epsilon_2 = 0.3$, respectively. Suppose the circuit parameters are selected as $R_1 = R_4 = 2\Omega$, $R_2 = 3\Omega$, $R_3 = 1\Omega$, $C_1 = 0.3F$. Then, the system parameters can be written as

$$\begin{aligned}
 A_1 &= \begin{bmatrix} 1 - 1.2927\epsilon_1 & 0.9921\epsilon_1 \\ 0.4252 & 0.7165 \end{bmatrix}, \\
 A_2 &= \begin{bmatrix} 1 - 1.2927\epsilon_2 & 0.9921\epsilon_2 \\ 0.4252 & 0.7165 \end{bmatrix}, \\
 B_1 &= \begin{bmatrix} -0.1247\epsilon_1 \\ -0.1417 \end{bmatrix}, B_2 = \begin{bmatrix} -0.1247\epsilon_2 \\ -0.1417 \end{bmatrix}, \\
 D_1 &= \begin{bmatrix} -0.1247\epsilon_1 \\ -0.1417 \end{bmatrix}, D_2 = \begin{bmatrix} -0.1247\epsilon_2 \\ -0.1417 \end{bmatrix}.
 \end{aligned}$$

The matrix Ψ is selected as:

$$\Psi = \begin{bmatrix} 0.3 & 0.7 \\ 0.8 & 0.2 \end{bmatrix}.$$

In addition, the other parameter and external disturbance are

given, respectively, as $\zeta = 0.1$ and

$$w(k) = 0.1\sin(k).$$

Under the case of quantized signals, the quantization range and coding length are set as $\Lambda = 3.2$ and $X = 3$ bits. It is calculated as $\Theta = 0.4$ by the formula $\Theta = \Lambda/2^X$. By solving the LMIs in Theorem 1, we can obtain $\theta_2 = 0.6250$, $\lambda_{min}(P) = 1.5135$ and $\lambda_{max}(P) = 2.1665$ to satisfy the condition of Definition 1. The control gains are obtained as follows:

$$\begin{aligned}
 K_1 &= [3.3622 \ 2.3501], \\
 K_2 &= [3.8539 \ 2.5227].
 \end{aligned}$$

We set the initial state as $x(0) = [0 \ 0]^T$, set $\bar{j}_i = 2$ and establish a maximum coding range of $\Lambda_{max} = 12.8000$ to encompass the state signal. The coding length of $\tilde{\mu}(k)$ is set to $Y = 2$ bits. Then, the parameter $\bar{l}_i = 1$ can be obtained from (17) and (23), and the minimum error is $\Theta\phi_{min} = 0.2$. Fig. 3 and Fig. 4 show the open-loop and closed-loop state trajectories, respectively. From the simulation plots, it is evident that the open-loop state trajectories diverge rapidly under the influence of bound perturbation inputs whereas the closed-loop state trajectories remain bound.

The trajectory plots of the closed-loop system's state for various coding lengths are presented in Fig. 4, where $x(k)$ and $\bar{x}(k)$ correspond to coding lengths $Y = 2$ and $Y = 4$, respectively. Fig. 5 depicts the trajectory of the control input based on the quantization signal, where $u(k)$ and $\bar{u}(k)$ correspond to coding lengths $Y = 2$ and $Y = 4$, respectively. The figure illustrates that the convergence region with a smaller coding length is larger compared to that with a larger coding length. Thus, coding length significantly impacts system performance. Fig. 6 shows the trajectory plots of the system state error $e_2(k)$, $e_3(k)$, and $e_4(k)$ before and after encoding and decoding for encoding lengths $X = 2, 3, 4$. It is observed that a larger packet length reduces the convergence region of the system state due to unavoidable errors, which adversely affect system performance. In essence, a larger coding length mitigates the impact of errors before and after coding and decoding, thereby enhancing system performance.

V. CONCLUSION

This work investigated the problem of input-to-state stabilization of discrete-time MJSs. A quantized control scheme involving coding and decoding procedures was proposed. The relationship between the error in the system state before and after encoding and decoding, the quantization range, and the packet length was established in (23). A criterion on ISS of the quantized closed-loop system was presented in Theorem 1, utilizing a Lyapunov function and the Schur complement. The gains of the required quantized controller can be obtained from a feasible solution of LMIs (25), (31), and (32). Finally, the proposed method was validated using an operational amplifier circuit system. Since network systems share data transmission links and are vulnerable to attacks, communication security is crucial. Future work should explore how to integrate data encryption with the encoding and decoding procedures.

REFERENCES

- [1] L. Yao, Z. Wang, X. Huang, Y. Li, Q. Ma, and H. Shen, "Stochastic sampled-data exponential synchronization of Markovian jump neural networks with time-varying delays," *IEEE Transactions on Neural Networks and Learning Systems*, vol. 34, no. 2, pp. 909–920, 2023.
- [2] X. Qin, J. Dong, J. Zhou, and T. Jiang, "Designing asynchronous filter with uncertain conditional probabilities for periodic discrete-time Markov jump systems," *Communications in Nonlinear Science and Numerical Simulation*, vol. 121, p. 107242, 2023.
- [3] F. Xu and C. Wei, "Stability of nonlinear semi-Markovian switched stochastic systems with synchronously impulsive jumps driven by G-Brownian motion," *IAENG International Journal of Computer Science*, vol. 50, no. 2, pp. 778–784, 2023.
- [4] K. Loparo and F. Abdel-Malek, "A probabilistic approach to dynamic power system security," *IEEE Transactions on Circuits and Systems*, vol. 37, no. 6, pp. 787–798, 1990.
- [5] T. Sathyan and T. Kirubarajan, "Markov-jump-system-based secure chaotic communication," *IEEE Transactions on Circuits and Systems I: Regular Papers*, vol. 53, no. 7, pp. 1597–1609, 2006.
- [6] A. Serletis and L. Xu, "Markov switching oil price uncertainty," *Oxford Bulletin of Economics and Statistics*, vol. 81, no. 5, pp. 1045–1064, 2019.
- [7] F. Zuhairroh, D. Rosadi, and A. R. Effendie, "Multi-state discrete-time Markov chain SVIRS model on the spread of COVID-19," *Engineering Letters*, vol. 30, no. 2, pp. 598–608, 2022.
- [8] J. N. A. Bueno, L. B. Marcos, K. D. Rocha, and M. H. Terra, "Regulation of uncertain Markov jump linear systems with application on automotive powertrain control," *IEEE Transactions on Systems, Man, and Cybernetics: Systems*, vol. 53, no. 8, pp. 5019–5031, 2023.
- [9] X.-L. Zhang, H.-L. Li, Y. Yu, L. Zhang, and H. Jiang, "Quasi-projective and complete synchronization of discrete-time fractional-order delayed neural networks," *Neural Networks*, vol. 164, pp. 497–507, 2023.
- [10] F.-L. Lian, J. Moyne, and D. Tilbury, "Network design consideration for distributed control systems," *IEEE Transactions on Control Systems Technology*, vol. 10, no. 2, pp. 297–307, 2002.
- [11] Z. Tian, S. Li, Y. Wang, and B. Gu, "Priority scheduling of networked control system based on fuzzy controller with self-tuning scale factor," *IAENG International Journal of Computer Science*, vol. 44, no. 3, pp. 308–315, 2017.
- [12] J.-Y. Li, Z. Wang, R. Lu, and Y. Xu, "Distributed filtering under constrained bit rate over wireless sensor networks: Dealing with bit rate allocation protocol," *IEEE Transactions on Automatic Control*, vol. 68, no. 3, pp. 1642–1654, 2023.
- [13] E. J. Msechu and G. B. Giannakis, "Sensor-centric data reduction for estimation with WSNs via censoring and quantization," *IEEE Transactions on Signal Processing*, vol. 60, no. 1, pp. 400–414, 2012.
- [14] Z. Yan, D. Zuo, T. Guo, and J. Zhou, "Quantized \mathcal{H}_∞ stabilization for delayed memristive neural networks," *Neural Computing and Applications*, vol. 35, no. 22, pp. 16473–16486, 2023.
- [15] Y. Zhou, X.-H. Chang, and J. H. Park, "Quantized filtering for switched memristive neural networks against deception attacks," *Journal of the Franklin Institute*, vol. 361, no. 10, p. 106883, 2024.
- [16] Y. Liu, F. Fang, J. H. Park, H. Kim, and X. Yi, "Asynchronous output feedback dissipative control of Markovian jump systems with input time delay and quantized measurements," *Nonlinear Analysis: Hybrid Systems*, vol. 31, pp. 109–122, 2019.
- [17] N. Yang, D. Chen, and J. Hu, "Quantised control of delayed Markovian jump systems with partly known transition probabilities," *IET Control Theory & Applications*, vol. 15, no. 3, pp. 372–389, 2021.
- [18] G. Zong and H. Ren, "Guaranteed cost finite-time control for semi-Markov jump systems with event-triggered scheme and quantization input," *International Journal of Robust and Nonlinear Control*, vol. 29, no. 15, pp. 5251–5273, 2019.
- [19] J. Zhou, J. Dong, S. Xu, and C. K. Ahn, "Input-to-state stabilization for Markov jump systems with dynamic quantization and multimode injection attacks," *IEEE Transactions on Systems, Man, and Cybernetics: Systems*, vol. 54, no. 4, pp. 2517–2529, 2024.
- [20] Z. Wang, L. Wang, S. Liu, and G. Wei, "Encoding-decoding-based control and filtering of networked systems: Insights, developments and opportunities," *IEEE/CAA Journal of Automatica Sinica*, vol. 5, no. 1, pp. 3–18, 2018.
- [21] S. Dey, A. Chiuso, and L. Schenato, "Linear encoder-decoder-controller design over channels with packet loss and quantization noise," in *2015 European Control Conference (ECC)*. Linz, Austria: IEEE, July 2015, pp. 934–939.
- [22] Y. Song, Z. Wang, L. Zou, and S. Liu, "Endec-decoder-based N-step model predictive control: Detectability, stability and optimization," *Automatica*, vol. 135, p. 109961, 2022.
- [23] M. Wakaiki, "Self-triggered stabilization of discrete-time linear systems with quantized state measurements," *IEEE Transactions on Automatic Control*, vol. 68, no. 3, pp. 1776–1783, 2023.
- [24] Y. Tao, H. Tao, Z. Zhuang, V. Stojanovic, and W. Paszke, "Quantized iterative learning control of communication-constrained systems with encoding and decoding mechanism," *Transactions of the Institute of Measurement and Control*, vol. 46, no. 10, pp. 1943–1954, 2024.
- [25] J. Li, Y. Niu, and D. W. Ho, "Limited coding-length-based sliding-mode control with adaptive quantizer's parameter," *IEEE Transactions on Automatic Control*, vol. 67, no. 9, pp. 4738–4745, 2022.
- [26] M. Sathishkumar, R. Sakthivel, C. Wang, B. Kaviarasan, and S. M. Anthoni, "Non-fragile filtering for singular Markovian jump systems with missing measurements," *Signal Processing*, vol. 142, pp. 125–136, 2018.
- [27] S. Dong, L. Liu, G. Feng, M. Liu, Z.-G. Wu, and R. Zheng, "Cooperative output regulation quadratic control for discrete-time heterogeneous multiagent Markov jump systems," *IEEE Transactions on Cybernetics*, vol. 52, no. 9, pp. 9882–9892, 2022.
- [28] X. Qin, J. Dong, X. Zhang, T. Jiang, and J. Zhou, " \mathcal{H}_∞ control of time-delayed Markov jump systems subject to mismatched modes and interval conditional probabilities," *Arabian Journal for Science and Engineering*, vol. 49, no. 5, pp. 7471–7486, 2024.
- [29] J. Han, Z. Zhang, X. Zhang, and J. Zhou, "Design of passive filters for time-delay neural networks with quantized output," *Chinese Physics*

- B*, vol. 29, no. 11, p. 110201, 2020.
- [30] X. Qu, X. Li, and X. Cao, "Quantized adaptive bounded-H-infinity tracking control for a class of stochastic nonaffine nonlinear systems," *IAENG International Journal of Applied Mathematics*, vol. 52, no. 2, pp. 298–307, 2022.
- [31] J. Dong, X. Ma, X. Zhang, J. Zhou, and Z. Wang, "Finite-time \mathcal{H}_∞ filtering for Markov jump systems with uniform quantization," *Chinese Physics B*, vol. 32, no. 11, p. 110202, 2023.
- [32] B. Wu, X.-H. Chang, and X. Zhao, "Fuzzy \mathcal{H}_∞ output feedback control for nonlinear NCSs with quantization and stochastic communication protocol," *IEEE Transactions on Fuzzy Systems*, vol. 29, no. 9, pp. 2623–2634, 2021.
- [33] J. Song and X.-H. Chang, "Induced \mathcal{L}_∞ quantized sampled-data control for T-S fuzzy system with bandwidth constraint," *IEEE Transactions on Fuzzy Systems*, vol. 31, no. 3, pp. 1031–1040, 2023.
- [34] J. Zhou, J. Dong, and S. Xu, "Asynchronous dissipative control of discrete-time fuzzy Markov jump systems with dynamic state and input quantization," *IEEE Transactions on Fuzzy Systems*, vol. 31, no. 11, pp. 3906–3920, 2023.
- [35] K. Zhou and P. P. Khargonekar, "Robust stabilization of linear systems with norm-bounded time-varying uncertainty," *Systems & Control Letters*, vol. 10, no. 1, pp. 17–20, 1988.
- [36] S. Boyd, L. El Ghaoui, E. Feron, and V. Balakrishnan, *Linear Matrix Inequalities in System and Control Theory*. Philadelphia: SIAM, 1994.
- [37] E.-K. Boukas, *Control of Singular Systems with Random Abrupt Changes*. Springer Science & Business Media, 2008.
- [38] S. Andrea, R. Marco, A. Terry, C. Francesca, C. Jessica, G. Debora, S. Michaela, and T. Stefano, *Global Sensitivity Analysis: The Primer*. John Wiley & Sons, 2008.
- [39] J. Song, Y. Niu, and H.-K. Lam, "Reliable sliding mode control of fast sampling singularly perturbed systems: A redundant channel transmission protocol approach," *IEEE Transactions on Circuits and Systems I: Regular Papers*, vol. 66, no. 11, pp. 4490–4501, 2019.